www.cadanda.com
Computer-Aided Design AND APPLICATIONS

Towards a Foot Bio-model for Performing Finite Element Analysis for Footwear Design Optimization using a Cloud Infrastructure

Zoi Koutkalaki[1], Panagiotis Papagiannis[2], Philip Azariadis[3], Paraskevas Papanikos[4], Sofia Kyratzi[5], Dimitrios Zissis[6], Dimitris Lekkas[7] and Elias Xidias[8]

[1]University of the Aegean, zoikout@aegean.gr
[2]University of the Aegean, papagiannis@aegean.gr
[3]University of the Aegean, azar@aegean.gr
[4]University of the Aegean, ppap@aegean.gr
[5]University of the Aegean, skiratzi@syros.aegean.gr
[6]University of the Aegean, dzissis@aegean.gr
[7]University of the Aegean, dlek@aegean.gr
[8]University of the Aegean, xidias@aegean.gr

ABSTRACT

This paper presents current research results that concern the generation of foot bio-models for performing finite element analysis for footwear design evaluation and optimization. The foot bio-models produced so far include complete geometric models of the foot bones along with their corresponding material properties. For the generation of the bones geometry a dense set of CT scan data is utilized. Four different approaches for the reconstruction of the corresponding 3D surfaces are presented and discussed. A preliminary FE analysis for simulating foot/ground interaction has been carried out to assert the performance of the chosen material type and properties. Finally, a cloud infrastructure is introduced to provide to the end-users a web-based interface for performing simulation scenarios concerning foot/footwear and foot/ground interaction.

Keywords: foot bio-model, foot FEM model, foot FEA, foot materials, footwear design, footwear materials, cloud application.

1. INTRODUCTION

The Evolution of computer-aided design applications in combination with advancements in medical imaging technologies and reverse engineering techniques, have formed the foundations for the development of the integrated field of bio-CAD in order to support biomedical engineering. Bio-CAD is mainly related to the creation of anatomic models of human soft and hard tissues that can be extensively used in diagnostic and therapeutic medical applications [28]. In particular, the produced 3D bio-models replicate the geometry and shape of the physical structure in computer-based form and can be employed for visualization, biomedical analysis and simulation purposes [19].

Nowadays, the Finite Element Method (FEM) is a widely used tool for computing several parameters affecting foot biomechanics, such as internal stresses and strain states of the foot-angle complex, and the load distribution between foot and footwear during gait. Finite Elements Analysis (FEA) allows for making adjustments to the shape and the materials selection of footwear without the need to pass through time-consuming trial and error cycles involving physical prototypes. On the other hand, FEM results rely heavily on the accuracy of the underlying bio-model that it is used to represent the actual human foot, the selection of the materials and the determination of the various loads and boundary conditions [3].

The work presented in this paper is part of a research project focusing on the development of cost-effective and accurate computer-aided design and engineering (CAD/CAE) tools for the determination and optimization of design parameters used for the production of comfort footwear (project acronym: OPT-SHOES). In particular, this research focuses on technologies and methodologies for determining and

Taylor & Francis

optimizing the following footwear related functionalities: fitting, shock absorption, foot plantar pressure distribution and bending/torsion. The determination and optimization of these parameters necessitates the development of (a) highly-accurate foot and shoe models, (b) appropriate FEM of the foot and shoe components, and (c) highly-accurate simulation tools based on human behavioral models for performing FEA. An added goal of OPT-SHOES it to make the entire solution available to the end-user through a cloud based architecture. This benefits end users by eliminating the requirement of investing on expensive software and hardware.

This paper consists of two main parts. The first part focuses on the geometric reconstruction of the foot bones and the second part on the interaction of foot/footwear and ground and on the architecture design of the associated cloud application. In the first part, the production of a foot bio-model from dense CT scans, including the corresponding material properties for hard and soft tissues is presented. Our aim is to critically review existing methodologies in the current state of the art by pointing out crucial phases, problems and/or difficulties. This is done by following four reconstruction approaches, where two commercial software suites and two methods based on Poisson surface reconstruction are employed (see Section 2). The resulting foot bio-models are evaluated based on their applicability for simulation purposes with FEA. In the second part of the paper, we focus on the foot/footwear and ground interaction where a set of material properties for the footwear and ground structures has been developed (see Section 3). These materials are tested in a preliminary FE analysis, which is presented in Section 4. Finally, the proposed cloud architecture showing the internal and external interactions between the OPT-SHOES system components is presented in detail in Section 5.

2. HUMAN FOOT RECONSTRUCTION

The human foot consists of 26 bones, 33 joints and various muscles, ligaments and tendons along with soft tissues like vessels, nerves, and the skin. With regard to the human body planes and the directional terms employed by medical practitioners, six foot sides are distinguished (Fig. 1): the medial (or big toe) side, the lateral (or little toe) side, the distal side that is the side away from the foot center, the proximal side that is close to the foot center, the anterior (or front side) and the posterior (or back) side. In addition, there are the dorsal and the plantar surfaces of the foot.

The construction of human soft and hard tissue bio-models is considered in a reverse engineering framework as a reconstruction process that is based on non-invasive imaging techniques. Computed Tomography (CT), Magnetic Resonance Imaging (MRI) and Ultrasonography are frequently used for this purpose since they provide structural information, physical properties and geometric data of human body through a series of tomographic images. The different capacity of each technique to penetrate human hard and soft tissues underline a tissue oriented acquisition process that is highly associated to the desired degree of resolution of the produced tissue images [20].

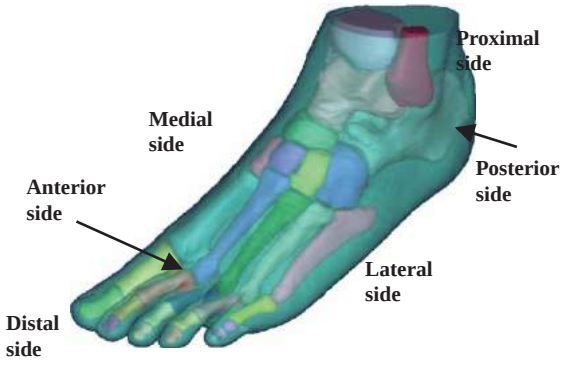

Fig. 1: The main directional sides of a foot.

2.1. Geometric Modeling of the Foot Bones

In the last thirty years significant research efforts have focused on three-dimensional rebuilding of bio-models from (CT) and (MRI) data. The main steps for the construction of a 3D bio-model include (i) image acquisition, (ii) image processing and (iii) the 3D reconstruction of the tissue. Image processing involves image segmentation to regions of interest that best describe the boundaries and the inner parts of the tissue to be constructed. Every pixel of each image takes grayscale values which are interpreted as different intensity values. Segmentation of medical images is a difficult task due to the complexity of human tissues, image noise, and the ambiguity of image data that frequently includes pixels with overlapping or close scalar values, resulting in an inaccurate representation of tissue contours [8]. Currently, semi-automated segmentation approaches are preferred, which employ processing methods such as the snake technique [13] and the edge-based segmentation [31] combined with a manual intervention mainly in pre-processing stage for the image thresholding and in post-processing stage for further image readjustments.

In this work, a complete reconstruction of foot bones from dense CT scans using four different approaches is presented. The first approach is based on the commercial software MIMICS. The second follows a Reverse Engineering (RE) methodology where a point-cloud is extracted from CT scans for each bone. Then, basic RE techniques are applied to reconstruct the bone surface by using the commercial software Geomagic. The last two approaches implement the

Poisson surface reconstruction method [15,16]. The purpose of this section is to highlight the difficulties and the most critical phases of each reconstruction process and to evaluate the resulting foot bio-models with respect to their applicability for FE analysis.

2.1.1. *Bones reconstruction through MIMICS*

Foot data used in this research is based on a set of CT scans taken on a foot of a healthy male subject with a resolution of 0.5 mm. There are about 800 different foot sections in the available dataset. The main tasks and difficulties during the reconstruction process are focused on image segmentation. More specifically, the boundaries and the included area of each bone are determined in every section in a semi-automatic way. This is the most difficult and critical part of the reconstruction process since it requires extensive manual work and knowledge of the human foot anatomy. This process is performed by defining a mask for each bone. This mask is used to segment intensity values in every section. Given the set of masks for each bone the software is able to perform 3D surface reconstruction using a boundary representation (mesh).

An example of this process is given in Fig. 2 where the reconstruction process of the ankle bone is depicted. The process is initiated by the identification of the angle bone in each CT section (Fig. 2(a)). Then a mask is created (Fig. 2(b)) and improved (Fig. 2(c)) to reflect the boundary and the included area of the bone. This process is repeated for each CT section where the ankle bone is identified. Then the software produces a 3D surface model of the identified bone (Fig. 2(d)). Failing in manually determining the correct interior part of the bone will result to wrong bone geometric reconstruction.

2.1.2. *Bones reconstruction through a reverse engineering approach*

Given the segmented image sections that are produced from the previous process a point-cloud is generated for each one of the foot bones. The point-cloud is generated by sampling the boundaries of the mask on the corresponding image sections. Putting the sampled points along an axis following a 0.5 mm interval, one is able to obtain a point-cloud for each bone. The main goal of this approach is to produce a surface model of each bone based on the corresponding point-cloud data. This is a typical reverse engineering (RE) approach which consists of the following basic phases [29]: (a) data pre-processing, (b) parameterization and surface generation (mesh) and (c) surface smoothing. These phases have been realized through the commercial software Geomagic.

Pre-processing concerns the removal of noisy data and possible outliers in the point-cloud. Usually, the point-cloud produced from the previous procedure doesn't contain noisy data and/or outliers. Surface generation concerns the production of a three-dimensional triangle mesh of the cloud surface. Care has to be taken in order to remedy triangles with wrong orientation or ill geometry (too small ankles or spikes). Local remeshing techniques and surface smoothing are commenced to eliminate these artifacts. The tradeoff in this step is that the smoother the resulted surface the less approximates the original point-cloud.

The aforementioned reverse engineering process is depicted in Fig. 3 with the ankle bone example. The initial point-cloud is given in Fig. 3(a) while the result of the mesh generation is depicted in Fig. 3(b). All data points are vertices of the generated triangle mesh so the reconstruction error in this phase can be regarded as equal to zero. Fig. 3(c) depicts the surface resulted after the application of a smooth operation. The new surface is smoother and free from ill triangle elements, and approximates the original data with a ± 0.35 mm accuracy (Fig. 3(d)) which is acceptable for the purposes of this research.

2.1.3. *Bones reconstruction through the Poisson surface reconstruction method*

Poisson reconstruction is a global solution to the surface reconstruction problem that considers all the data at once. Here, the input data $\vec{V}$ are oriented points which consist of the original point-cloud and associated normal vectors that point inwards to the surface [15]. Poisson reconstruction creates smooth watertight surfaces that robustly approximate noisy data. However, it is not well suited for non-zero genus surfaces.

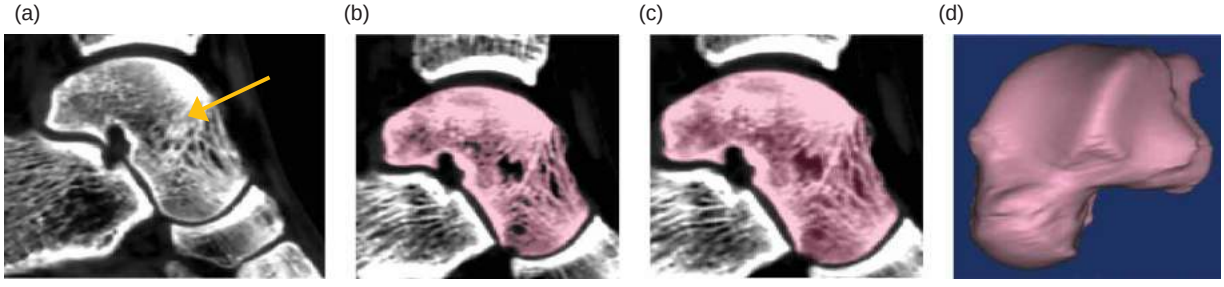

Fig. 2: The main phases of the ankle bone reconstruction process.

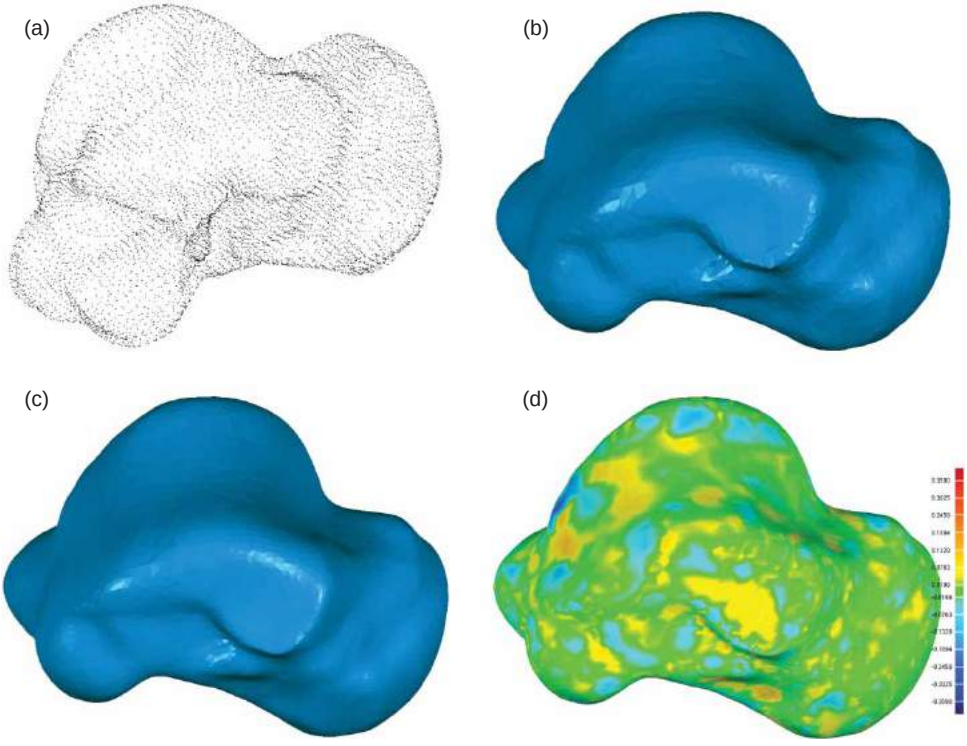

Fig. 3: The main phases of the ankle bone reverse engineering process.

In this method the problem of surface reconstruction is approximated using an implicit function framework. A 3D indicator function x is computed which is defined as 1 at points inside the model, and 0 at points outside. Then, the reconstructed surface (triangle mesh) is obtained by extracting an appropriate isosurface. The gradient of the indicator function is a vector field that is zero almost everywhere (since the indicator function is constant almost everywhere), except at points near the surface, where it is equal to the inward surface normal. Thus, the oriented point samples can be viewed as samples of the gradient of the model's indicator function. The problem of computing the indicator function thus reduces to finding the scalar function x whose gradient best approximates the vector field $\vec{V}$ defined by the samples. In mathematical formulation this problem is equivalent to $\min_x \|\nabla x - \vec{V}\|$ which can be transformed (by applying the divergence operator) to the Poisson problem $\Delta x = \nabla \cdot \nabla x = \nabla \cdot \vec{V}$. For an arbitrarily sample point $\mathbf{p}$, this problem can be also written as

$$E(x) = \int \|\nabla x(\mathbf{p}) - \vec{V}(\mathbf{p})\|^2 d\mathbf{p} \tag{2.1}$$

The scalar indicator function is represented in an adaptive octree and it is iso-contoured using an adaptive marching cubes algorithm. Details on this method can be found in the work of Kazhdan et al. [15].

In order to apply this method to our foot-bones reconstruction problem the required set of oriented data should be produced out of the original point-cloud. The main sub-problems in this task are, first, to produce accurate normal vectors and, then, to ensure their consistent orientation. These issues are tackled in the next subsection.

2.1.3.1. Generation of oriented data. The focus of this section is on the production of the necessary oriented data $\vec{V}$. For the calculation of the normal vectors $\mathbf{n}_i \in \mathbb{R}^3, i \in \{1, \ldots, N\}$ a moving least squares approach has been used according to [1]. Let $\mathbf{p}_i \in \mathbb{R}^3, i \in \{1, \ldots, N\}$ be the cloud points, $\mathbf{r}_j, j \neq i$ be the point of interest and $\mathbf{n}$ the corresponding normal vector. A local support plane H is considered that passes through $\mathbf{r}_j$. This plane is computed by minimizing the weighted distances of the points $\mathbf{p}_i$ to H. The weights are computed from the distances of $\mathbf{p}_i$ to $\mathbf{r}_j$ using a smooth, positive, monotone decreasing function $\theta = \frac{1}{1+\|\mathbf{p}_i - \mathbf{r}_j\|}$. In this way, a weighted least squares problem is formulated which is solved by minimizing

$$\sum_{i=1}^{N} [\mathbf{n} \cdot (\mathbf{p}_i - \mathbf{r}_j)]^2 \theta(\|\mathbf{p}_i - \mathbf{r}_j\|) \tag{2.2}$$

In bilinear form Eqn.(2.2) can be rewritten as

$$\min_{\|\mathbf{n}\|=1} \mathbf{n}^{\mathrm{T}} \mathrm{B} \mathbf{n} \tag{2.3}$$

where B = $\{b_{kl}\}$ is the weighted co-variance matrix

$$b_{kl} = \sum_{i=1}^{N} \theta(p_{ik} - r_{jk})(p_{il} - r_{jl}) \tag{2.4}$$

The required normal vector corresponds to the eigenvector of B with the smallest eigenvalue. The normal vectors produced from the above procedure need to be oriented in a consistent way in order to ensure an oriented dataset $\vec{V}$ as input for the reconstruction method. For the normals orientation we have used the Euclidean Minimum Spanning Tree (EMST) [9]. In this method, a connected graph is formulated with edge cost equal to $1 - |\mathbf{n}_i \cdot \mathbf{n}_j|$, which expresses the cost of propagating the orientation of $\mathbf{n}_i$ to its neighboring normal vector $\mathbf{n}_j$. A propagation order can be achieved by traversing the minimal spanning tree (MST) of the resulting graph. This propagation order favors normal vectors which are almost parallel and has proven to be more robust compared to the propagation based on Euclidean proximity.

2.1.3.2. Example. The applicability of the above methods to the ankle bone example (see point-cloud at Fig. 3(a)) is demonstrated in this subsection. Using the MLS method the normal vectors shown in Fig. 4(a) have been computed. Clearly, the normal vectors do not follow a consistent orientation. The normal vectors orientation is corrected by using the EMST method as it is shown in Fig. 4(b).

Having a set of oriented data $\vec{V}$ the application of Poisson reconstruction is feasible. Our implementation is based on a variant of the algorithm proposed in [15] which can be found in the CGAL library (www.CGAL.org). In this implementation the indicator function is constructed over a refined 3D Delaunay triangulation of the pointset instead of an adaptive octree. The most important variable in the reconstruction process is the "approximation distance" which determines the size and number of the tetrahedrals produced during the 3D Delaunay triangulation. A small value will result in the production of a detailed triangulation. This value is scaled according to the average distance of the point-cloud points and it has no effect on the final result when it is much smaller than the latter.

Three different cases of ankle bone reconstruction are depicted in Fig. 5 where the effect of the "approximation distance" parameter is visible. Larger values result to smoother surface reconstructions with smaller number of triangles but with a higher deviation from the original dataset, as it is shown in the "Avrg. Error" parameter.

2.1.3.3. Bones reconstruction through the screened Poisson surface reconstruction method. Although with the previous method we were able to handle almost all foot bones, in some cases the method failed to produce adequate results. For example, the shank bone has a flat upper area corresponding to the boundaries of the effective area of the CT scanner. This flat area is not reconstructed accurately as it is shown in Fig. 6(a). With the screened Poisson surface reconstruction method, which is reviewed in this subsection, we were able to solve this issue as it is shown in Fig. 6(b).

In [16] the initial Poisson reconstruction method has been revised to explicitly incorporate the data points as interpolation constraints. In the revised method data fidelity terms are used to "screen" the associated Poisson equations. These screening terms correspond to a soft constraint that encourages the reconstructed isosurface to pass through the input points. More specifically, the set of input points $P = \{\mathbf{p}_i\}$ is associated with weights $w : P \to \mathbb{R}^+$. Then a new soft term is incorporated to the problem (2.1) that

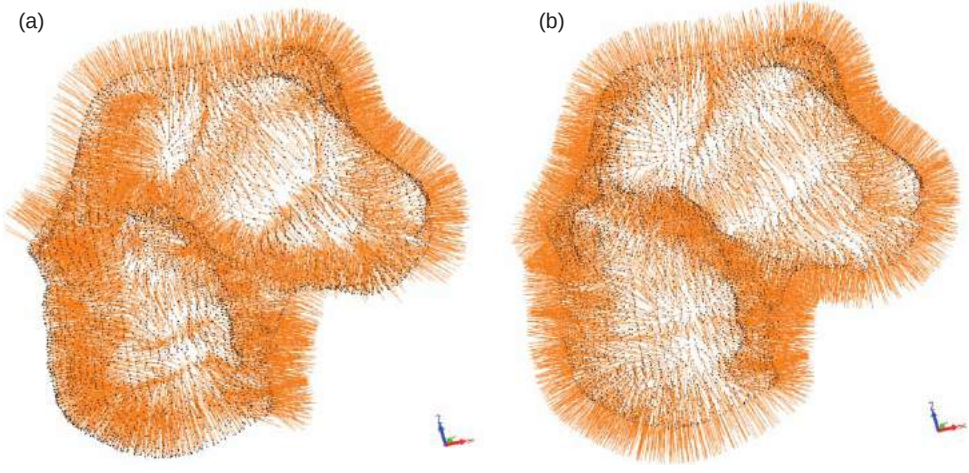

Fig. 4: (a) The initial and (b) the final normal vectors orientation.

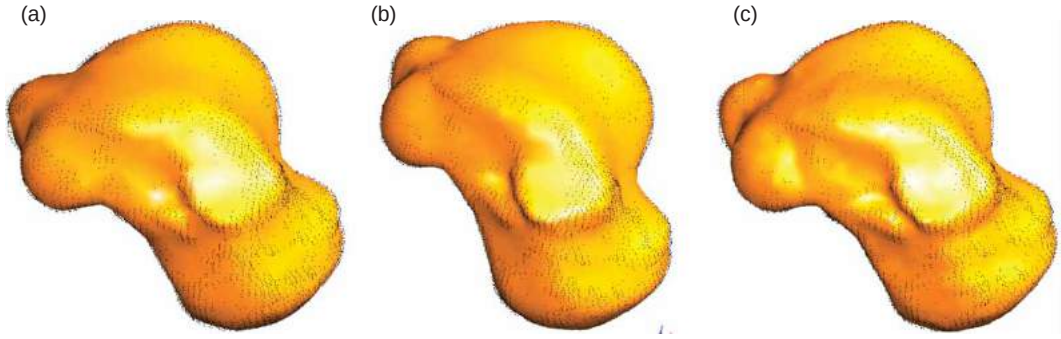

Fig. 5: Reconstructions of the ankle bone using the Poisson method and different values of the approx. distance parameter.

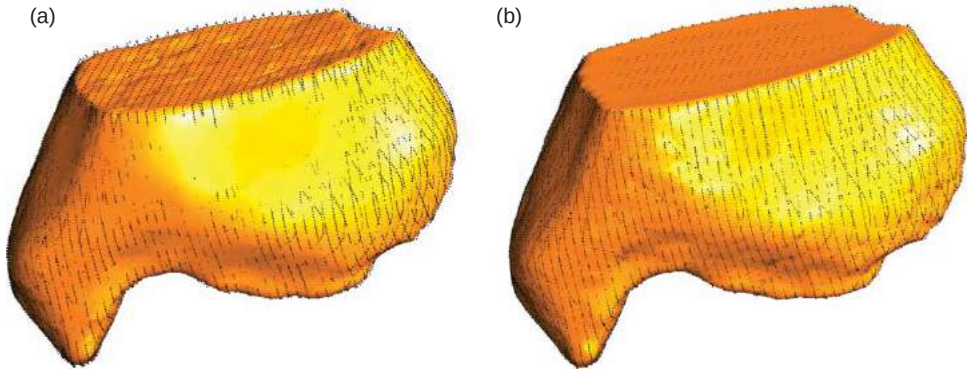

Fig. 6: Reconstructions of the shank bone using (a) the original and (b) the screened Poisson surface reconstruction method. Clearly, the original method fails to reproduce accurately flat bone areas.

penalizes the function's deviation at the data points:

$$E(x) = \int \|\nabla x(\mathbf{p}) - \vec{V}(\mathbf{p})\|^2 d\mathbf{p} + \frac{a \cdot \text{Area}(P)}{\sum_{\mathbf{p}\in P} w(p)} \sum_{\mathbf{p}\in P} w(\mathbf{p}) x^2(\mathbf{p}) \tag{2.5}$$

where a is a weight that trades off the importance of fitting the gradients and fitting the values, and Area(P) is the area of the reconstructed surface, estimated by computing the local sampling density as in [15]. The method is implemented using a conforming octree achieving a linear time complexity with respect to the number of data points. The authors have released the corresponding source code [14].

With the revised method we are able to (a) improve the reconstruction accuracy both globally and locally by incorporating confidence values to the data points, (b) to generate several versions of the bone surfaces according to the desired accuracy and smooth level. These features are important in our effort to derive the most appropriate FE model of the foot bones structure. With the revised method there is a large set of parameters that affect the quality and accuracy of the produced reconstructed surface. The most important parameter is the allowed octree depth which determines the depth at which the data point will be subdivided, which in turn determines the depth that the Poisson problem will be solved. A depth value d implies that the Poisson problem will be solved at octree depth $2^d \times 2^d \times 2^d$.

Three different surface reconstructions of the ankle bone are shown in Fig. 7 using different values for the octree depth. In all cases the data points have a weight factor equal to 4. At lower depth values the method produces a very smooth surface (see Fig. 7(a)-(b)). At depth value equal to 8 a very detailed surface reconstruction of the ankle bone is derived. In all cases the reconstruction accuracy is superior compared to the reconstructions of the original method.

2.1.4. *Final reconstruction of foot bones*

All four presented methodologies were able to generate 3D models of the foot bones. The complete foot bone models are depicted in Fig. 8. The commercial

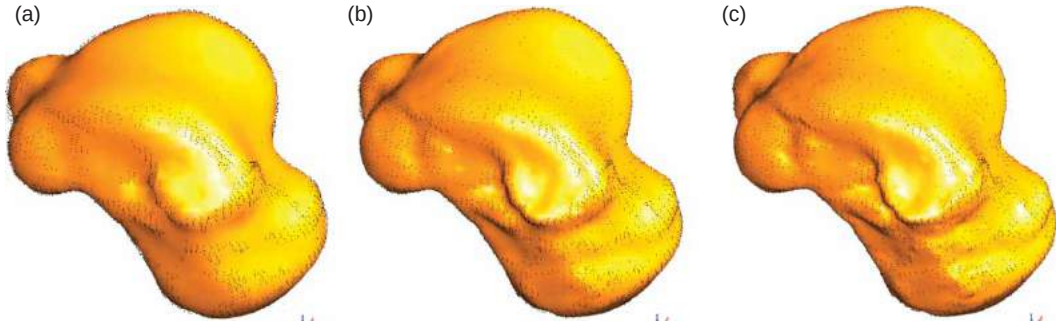

Fig. 7: Reconstructions of the ankle bone using different values of the octree depth parameter.

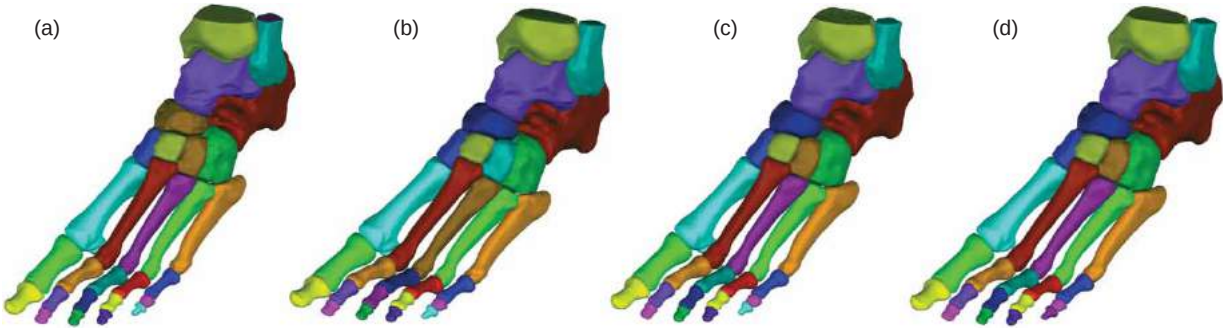

Fig. 8: Complete bio-models of the foot bones structure: (a) MIMICS result, (b) RE result, (c) Poisson method result and (d) Screened Poisson method result.

software produced highly accurate bone models with the cost of extensive manual work (see Fig. 8(a) and (b)). On the other hand, the Poisson reconstruction methods produced smoother surfaces and did not require any user interference. They work automatically as long as the required oriented pointset is provided. The generation of the oriented pointset out of the original point-cloud can also be done in an automatic way.

However, one has to bear in mind that the reconstructed bones will be used as an input for producing corresponding FE models for use in simulation purposes. Therefore, the encapsulation of small surface details like e.g. bone roughness is unnecessary and undesirable. For a successful FE model of a bone bio-model one has to balance between reconstruction accuracy and model complexity. For these reasons bio-models that provide enough accuracy and smoothness are favorable. In our case, for FEA experimentation we didn't use the third model due to the local accuracy problems denoted in Fig. 6. The selection of the most appropriate model for FE analysis depends on the pre-processing capabilities of the FEA software. If the pre-processor is unable to produce high-quality adaptive meshes with varying density then a smooth model like the one in Fig. 8(d) is advisable to be used. On the other hand, either one of the three models is an excellent base for a quality meshing.

2.2. Assignment of Material Properties for Foot Bio-models

Deciding on the mechanical properties of the hard and soft human tissues is an important part for the FEA systems involving the human foot. From the pioneering work of Katz in the 1970's (cited in [23], p102), to the recent work of Cheung and Zhang in 2006 [5] and to the present day, relevant data for human tissues have been documented and assigned to models of the human foot. Finite Elements Analysts of the human foot, tend to distinguish five distinct types of tissue, i.e., bones, ligaments, cartilage, plantar fascia and soft tissue. Though, anatomically not fully accurate (e.g. some very small and short skeletal muscles exist [14]), this view is considered a reasonable approximation to modeling the human foot. Up until now, hard tissue materials have been considered isotropic and linear-elastic, whereas soft tissues as materials possessing either a non-linear visco-elastic or hyperelastic behavior.

Component	Element type	Young's modulus E (MPa)	Poisson's ratio v	Cross Section (mm^2)
Bony structures	3D-tetrahedra	7300	0.3	
Soft tissue	3D-tetrahedra	Hyperelastic		
Cartilage	3D-tetrahedra	1	0.4	
Ligaments	Tension-only truss	260		18.4
Fascia	Tension-only truss	350		58.6

Tab. 1: Material Properties.

Table 1, cites material properties as used by Cheung and Zhang [5], Shariatmadari et al. [26] and that have been adopted for use in this research. The measured or estimated values for material properties by other researchers differ quite often depending on the method of measurement or theoretical model used respectively [3,10,24].

Bones are considered composite materials, consisting of cortical and trabecular tissue, each also considered a composite material in its own right [10]. Relevant mechanical models have been developed (see Oyen and Ferguson in [23]). The proposed Young's modulus and Poisson's ratio for the bones were assigned as 7300 MPa and 0.3, respectively, according to the human foot model developed by Gefen et al. [7]. These values were estimated by averaging the elasticity values of cortical and trabecular bones in terms of their volumetric contribution to the composite.

The Young's modulus of the cartilage [2,18], ligaments [27] and the plantar fascia [30] were selected from the literature. The ligaments and the plantar fascia are assumed to be tension only truss elements, while the cartilage is assigned with a Poisson's ratio of 0.4 for its nearly incompressible nature.

3. ASSIGNMENT OF MATERIAL PROPERTIES OF GROUND/FLOOR AND FOOTWEAR

The foot is expected to be in contact with the ground/floor (bare foot to ground contact) and the footwear (foot – footwear to ground contact). In many simulation cases the aim is to estimate the transfer of ground reaction forces to the foot, therefore the most significant part of footwear is the lower subassembly. A typical arrangement of parts for the lower subassembly is that of the outer or lower sole, the mid-sole and the in-sole. Optionally, in the footwear structure, consideration may be given to rigid heels, sole stiffening elements and sidewalls of the footwear upper. This paper, summarizes artificial materials, which account for most modern worldwide footwear production and are listed in Tab. 2.

Pure elastomers (e.g. polyisoprene rubber) are hyperelastic whereas the other materials are viscoelastic. However, Cheung and Zhang [5] have assumed isotropic and linear elastic properties for all materials rather than non-linear viscoelastic. On the other hand Lemmon et al. [17] have assumed isotropic hyperelastic behavior for PU (that are not pure hyperelastic materials) and other polymer foams, which is expressed with a third order polynomial. Currently, the linear and isotropic approach is followed, since a similar approach applies also to floor and human tissue materials.

The material choice for the floor and the ground is also important. Shariatmadari et al. [26] in their FE analysis of a human foot model, assumed that the floor (or ground) is homogeneous and isotropic material with Young Modulus equal to 209 GPa and Poisson's ratio equal to 0.3. With regard to the friction between the bare foot and the floor Cheung and Zhang [5] proposed a coefficient of dry friction equal to 0.6. The same coefficient is assumed with regard to the friction between the foot and single density PU insoles. On the other hand, when modeling poron insoles, Shariatmadari et al. [26] assumed a coefficient of dry friction equal to 0.1.

Material	Footwear Part	Young Modulus E (GPa)	Poisson Ratio ν	Density (g cm^{-3})
Natural (or isoprene) "rubber"	Out-sole	0.015–0.025	0.499	0.93
PU single density	Out-sole, mid-sole	0.04–0.12	0.26–0.33	0.7–1.15
PU double density	Out-sole	1.30–2.10	0.4–0.416	1.12–1.24
EVA	Mid-sole	0.01–0.04	0.47–0.49	0.945–0.955
PU foam	In-sole	0.01–0.03	0.23–0.33	1.12–1.24
ABS copolymer	Out-sole, heel, stiffening elements	11–29	0.391–0.422	1.01–1.21

Tab. 2: Footwear Material Assignment and Properties (at 20°C).

4. PRELIMINARY FE ANALYSIS OF FOOT/GROUND INTERACTION

We have used a simplified 3D bio-model of the foot which consists of the bony structure and the soft tissue structure that are assumed bonded for these trial runs. The goal of the trial runs was to investigate the convergence of the model with respect to non-linear material models for the soft tissue and the sole material modeled as a flat pad (see Fig. 9). Three different foot positions, corresponding to three gait positions, were modeled and the maximum plantar pressure value was used in order to evaluate the proper load-step for the non-linear analysis. A combination of linear and non-linear material models were used according to Tab. 1, 2. Non-linear contact elements were used to model the interface between soft tissue and the sole. In all cases, the FE analysis converged to a feasible solution confirming the validity of the proposed material properties and models.

5. CLOUD APPLICATION

Model rendering and visualization software often comes with a heavy processing, storage and licensing cost that can be forbidding for many end users. To overcome this barrier various research proposals have attempted to provide remote visualization capabilities [11,22,12,6]. The term "remote visualization" generally refers to an architectural configuration where the visualization pipeline is partitioned such that some data within the pipeline crosses machine boundaries. According to Chen et al. [4] these approaches can be categorized by their architectural pipeline as (i) where the data, visualization processing and rendering occurs on the server, (ii) where data and visualization processing occurs on the server and (iii) where only the data resides on the server and the visualization processing, rendering and display occur at the end client.

Remote visualization faces many architectural challenges according to the chosen approach. While performing all visualization and rendering on the server and sending pre-rendered images to the end user benefits the user by avoiding any computation on his side, it often provides only a constrained navigation of the pre-rendered model. On the other hand, while maintaining only raw data on the server and requesting users perform all visualization and rendering on their machine does not suffer from such a restriction, it does put a heavy computational demand on end users. In this research approach, it is attempted to keep a balance between requirements and features; thus maintaining data and performing visualization-computation on the server, while sending end clients the geometry for rendering on their machine. This approach provides users with an unconstrained 3D navigation of models remotely

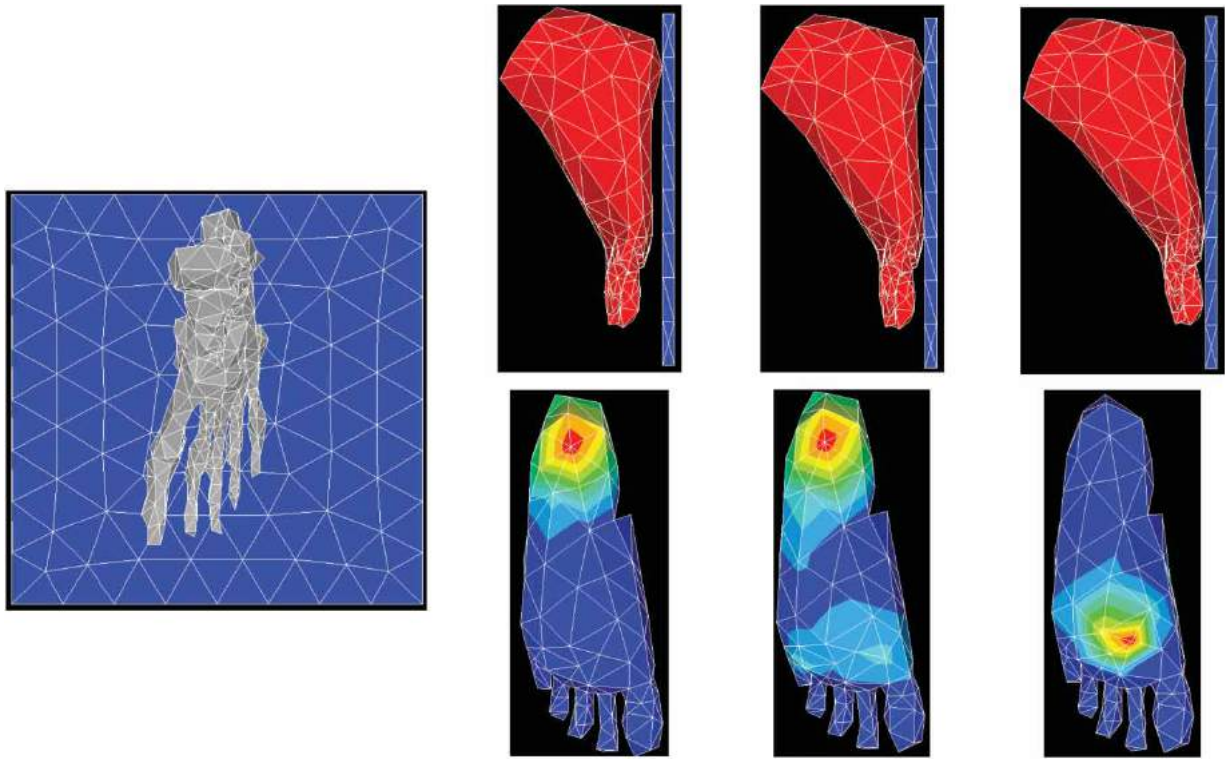

Fig. 9: Preliminary typical results of the FE analysis: positioning of the foot on a soft pad (left), modeling three cases and the resulting plantar pressure distribution (right).

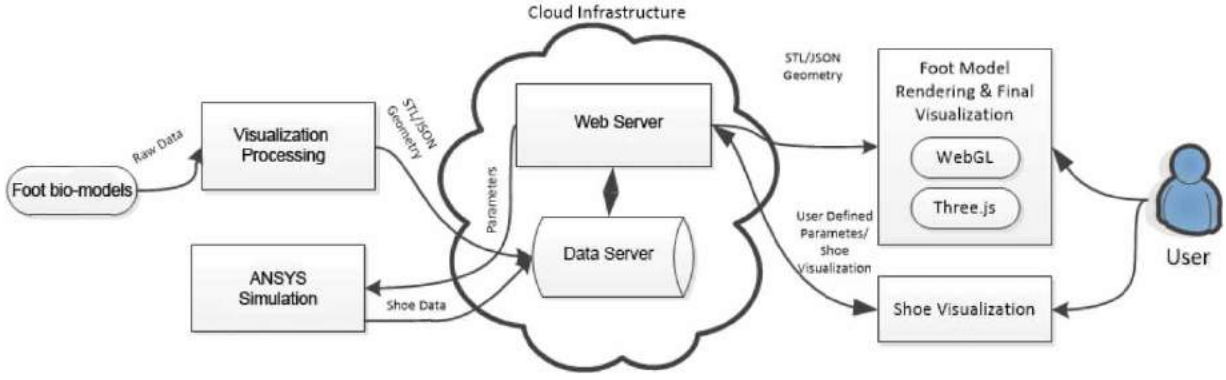

Fig. 10: High level conceptual design of the proposed architecture.

stored while avoiding creating any user performance bottlenecks.

Therefore, computational intensive processing is performed close to the data and intermediate visualization results for final rendering are send to the users. To increase the availability, reliability and performance of the infrastructure a cloud based architecture is employed. Cloud computing is a model for enabling convenient, on-demand network access, to a shared pool of configurable computing resources, (e.g., networks, servers, storage, applications, and services) that can be rapidly provisioned and released with minimal management effort or service provider interaction. In cloud computing, the available service models are [21]:

- *Infrastructure as a Service (IaaS).* This provides the capability to provision processing, storage, networks, and other fundamental computing resources, and allow the consumer to deploy and run arbitrary software, which can include operating systems and applications.
- *Platform as a Service (PaaS).* This provides the capability to deploy onto the cloud infrastructure, consumer-created or acquired applications, produced using programming languages and tools supported by the provider.
- *Software as a Service (SaaS).* This provides the capability to use the provider's applications running on a cloud infrastructure. The applications are accessible from various client devices, through a thin client interface, such as a web browser.

In this research cloud computing at an IaaS and PaaS level is applied. At IaaS level storage and operating resources are acquired while at a PaaS level ready-use-services are acquired. An overview of the designed Cloud infrastructure is given in Fig. 10, where:

- Foot bio-models are fed into the system as raw data from which visualization processing generates 3D models of the anatomy of the foot.
- The visualization results (geometry, textures, etc.) are successively uploaded to the cloud storage.
- Upon user request the visualization results are forwarded to the end client to be rendered on his/her machine through a cloud based web platform. Users are provided with unconstrained interaction of the 3D model.

An end user can request to perform a simulation on a number of shoe materials (according to user provided parameters). These are combined with foot bio-models and are passed for FE analysis to ANSYS. The simulation results are provided to the user via the web platform. An end user is delivered with visualization results which are rendered on the client Graphics Processing Unit with WebGL which is a JavaScript API that provides a way to execute shader code on a user's GPU. In addition we employ Three.js a lightweight cross-browser JavaScript library/API to animate and interact with 3D computer graphics in conjunction with WebGL.

6. CONCLUSIONS

In this paper, the most important steps performed so far towards developing a complete foot bio-model adequate for performing FE analysis with the combination of ground and/or footwear materials have been described. The goal is to deliver the final research results as an interactive tool based on Cloud infrastructure. Although, all produced bone bio-models can be utilized for the production of FE models, a smooth and accurate bio-model surface will ease the process of FE meshing and provide less complicated structures.

After extensive research, the most appropriate materials and their properties that can be applied to the construction of foot bio-models and for modeling the ground and footwear sole structures have been determined. Foot/ground and foot/footwear interactions depend heavily on the chosen materials and the preliminary results confirm that the proposed

material selection is capable of providing accurate simulation results.

The next steps of this research include the generation of the final FE model of all bone structures and corresponding FE models for the footwear sole structures that will be used for simulation purposes.

ACKNOWLEDGEMENTS

This research has been co-financed by the European Union (European Social Fund - ESF) and Greek national funds through the Operational Program "Education and Lifelong Learning" of the National Strategic Reference Framework (NSRF) - Research Funding Program "ARISTEIA". We'd like to thank Athens Euroclinic for providing us the foot CT dataset.

REFERENCES

[1] Adamson, A.; Alexa, M.: Approximating & Intersecting Surfaces from Points, Eurograhics Symposium on Geometry Processing, 2003, 230–239.

[2] Athanasiou, K. A.; Liu, G. T.; Lavery, L. A.; Lanctot, D. R.; Schenck, R.C.: Biomechanical topography of human articular cartilage in the first metatarsophalangeal joint, Clinical Orthopaedics, 348, 1998, 269–281, http://dx.doi.org/10.1097/00003086-199803000-00038

[3] Azariadis, P.:, Finite Element Analysis in Footwear Design, in The Science of Footwear, Editor Prof. Ravi Goonetilleke, Taylor & Francis Group, November 06, 2012, 321–337, http://dx.doi.org/10.1201/b13021-19

[4] Chen, J.; Yoon, I.; Bethel, W.: Interactive, internet delivery of visualization via structured prerendered multiresolution imagery, IEEE Transactions on Visualization and Computer Graphics, 14(2), 2008, 302–12. http://dx.doi.org/10.1109/TVCG.2007.70428

[5] Cheung, J. T.; Zhang, M.: A 3-Dimensional finite element model of the human foot and ankle for insole design, Arch. Phys. Med. Rehab. 86, 2005, 353–358. http://dx.doi.org/10.1016/j.apmr.2004.03.031

[6] Dupont, F.; Duval, T.; Fleury, C.; Forest, J.; Gouranton, V.; Lando, P.; Schmutz, A.: Collaborative Scientific Visualization: The COLLAVIZ Framework, In S. Coquillart, V. Interrante, & T. Kuhlen (Eds.), Joint Virtual Reality Conference of EuroVR - EGVE – VEC, 2010.

[7] Gefen, A.; Megido-Ravid, M.; Itzchak, Y.; Arcan, M.: Biomechanical analysis of the three-dimensional foot structure during gait: a basic tool for clinical applications, Journal of Biomechanical Engineering, 122, 2000, 630–639. http://dx.doi.org/10.1115/1.1318904

[8] Grove, O.; Rajab, K.; Piegl, A. L.; Lai-Yuen, S.: From CT to NURBS: Contour Fitting with B-spline Curves, Computer-Aided Design & Applications, 8(1), 2011, 3–21. http://dx.doi.org/10.3722/cadaps.2011.3-21

[9] Hoppe, H.; DeRose, T.; Duchamp, T.; McDonald, J.; Stuetzle, W.: Surface reconstruction from unorganized points, In Computer Graphics (Proc. SIGGRAPH '90), 1992, 26, 71–77.

[10] Huston, R. L.: Principles of Biomechanics, Dekker Mechanical Engineering Series, CRC Press, 2009, Boca Raton, Florida

[11] Jomier, J.; Jourdain, S.; Ayachit, U.; Marion, C.: Remote visualization of large datasets with MIDAS and ParaViewWeb, In Proceedings of the 16th International Conference on 3D Web Technology - Web3D'11, 2011, 147. New York, New York, USA: ACM Press. http://dx.doi.org/10.1145/2010425.2010450

[12] Jourdain, S.; Ayachit, U.; Geveci, B.: ParaViewWeb: A Web Framework for 3D Visualization and Data Processing, International Journal of Computer Information Systems and Industrial Management Applications, 3, 2011, 870–877.

[13] Kass, M.; Witkin, A.; Terzopoulos, D.: Snakes: Active Contour Models, International Journal of Computer Vision, 1988, 321–331. http://dx.doi.org/10.1007/BF00133570

[14] Kazhdan, M.; Bolitho, M.: Screened Poisson Surface Reconstruction Source Code, http://www.cs.jhu.edu/ misha/Code/PoissonRecon.

[15] Kazhdan, M.; Bolitho, M.; Hoppe, H.: Poisson Surface Reconstruction, Eurographics Symposium on Geometry Processing, 2006.

[16] Kazhdan, M.; Hoppe, H.: Screened Poisson Surface Reconstruction, ACM Trans. On Graphics, 32(3), 2013 (Presented at SIGGRAPH 2013.)

[17] Lemmon, D.; Shing, T. Y.; Hashmi, A.; Ulbrecht, J. S.; Cavanagh, P. R.: The Effect of Insoles in Theurapeutic Footwear – A finite Element Approach, Journal of Biomechanics, 30(6), 1997, 615–620. http://dx.doi.org/10.1016/S0021-9290(97)00006-7

[18] Liu, G. T.; Lavery, L. A.; Schenck, R. C.; Lanctot, D. R.; Zhu, C. F.; Athanasiou, K. A.: Human Articular Cartilage Biomechanics of the Second Metatarsal Intermediate Cuneiform Joint, The Journal of Foot & Ankle Surgery, 36(5), 1997, 336–374. http://dx.doi.org/10.1016/S1067-2516(97)80039-7

[19] Lohfeld, S.; Barron, V.; McHugh, P. E.: Biomodels of Bone: A Review, Annals of Biomedical Engineering, 33(10), 2005, 1295–1311. http://dx.doi.org/10.1007/s10439-005-5873-x

[20] Mehta, V. B.; Rajani, S.; Sinha, G.: Comparison of Image Processing Techniques (Magnetic Resonance Imaging, Computed Tomography Scan and Ultrasound) for 3D Modeling and Analysis

of the Human Bones, Journal of Digital Imaging, 10(1), 1997, 203–206. http://dx.doi.org/10.1007/BF03168701

[21] Mell, P.; Grance, T.: NIST SP 800–145. The NIST Definition of Cloud Computing (Draft), Recommendations of the National Institute of Standards and Technology, 2011.

[22] Moreland, K.; Rogers, D.; Greenfield, J.; Geveci, B.; Marion, P.; Neundorf, A.; Eschenberg, K.: Large scale visualization on the cray xt3 using paraview, In Cray User Group, 2011.

[23] Ochsner, A.; Ahmed, W. (eds): Biomechanics of Hard Tissues – Modeling, Testing and Materials, Wiley – VHC, 2010, Weinheim.

[24] Patil, K. M.; Braak, L. H.; Huson, A.: Analysis of stresses in two-dimensional models of normal and neuropathic feet, Medical & Biological Engineering & Computing, 34, 1996, 280–284. http://dx.doi.org/10.1007/BF02511238

[25] Putz, R.; Pabst, R. (eds): Sobotta – Atlas of Human Anatomy, Vol. 2, 14th edition, 2006, Elsevier GmbH, Munich.

[26] Shariatmadari, M. R.; English, R.; Rotwell, G.: Finite Element Study into the Effect of Footwear Temperature on the Forces Transmitted to the Foot during Quasi-Static Compression Loading, in IOP Conf. Series: Materials Science and Engineering 10(2010).

[27] Siegler, S.; Block, J.; Schneck, C. D.: The mechanical characteristics of the collateral ligaments of the human ankle joint, Foot & Ankle, 8, 1998, 234–242. http://dx.doi.org/10.1177/107110078800800502

[28] Sun, W.; Lal, P.: Recent development on computer aided tissue engineering - a review, Computer Methods and Programs in Biomedicine, 67(2), 2002, 85–103. http://dx.doi.org/10.1016/S0169-2607(01)00116-X

[29] Várady, T.; Martin, R. R.; Cox, J.: Reverse engineering of geometric models-an introduction, Computer-Aided Design, 29(4), 1997, 255–268. http://dx.doi.org/10.1016/S0010-4485(96)00054-1

[30] Wright, D.; Rennels, D.: A study of the elastic properties of plantar fascia, Journal of Bone and Joint Surgery, 1964, American Volume 46, 482–492.

[31] Ziou, D.; Tabbone, S.: Edge detection technique-An overview, Int. J. Pattern Recognit. Image Anal., 8, 1998, 537–559.